Terra Nova

WILEY

Terra Nova

RESEARCH ARTICLE OPEN ACCESS

Fe Oxidation State and Oxygen Isotope Composition of Diverse Metasomatized Peridotite Rocks

Federica Benedetti[1] | Giulia Marras[1] | Enrico Cannaò[2] | Gianluca Bianchini[3] | Daniele Brunelli[4] | Luigi Dallai[1,5] | Vincenzo Stagno[1,6]

[1]Department of Earth Sciences, Sapienza University of Rome, Roma, Italy | [2]Department of Earth Sciences "A. Desio", University of Milan, Milano, Italy | [3]Department of Physics and Earth Sciences, University of Ferrara, Ferrara, Italy | [4]Department of Chemical and Geological Sciences, University of Modena and Reggio Emilia, Modena, Italy | [5]National Institute of Geophysics and Volcanology (INGV), Rome, Italy | [6]National Institute of Geophysics and Volcanology (INGV), Palermo, Italy

Correspondence: Luigi Dallai (luigi.dallai@uniroma1.it) | Vincenzo Stagno (vincenzo.stagno@uniroma1.it)

Received: 19 September 2024 | **Revised:** 6 February 2025 | **Accepted:** 1 July 2025

Keywords: ferric iron | metasomatism | oxygen isotopes | spinel | synchrotron Mössbauer | Tallante

ABSTRACT

Metasomatic fluids are thought to be oxidising agents that react with the surrounding mantle rocks, causing changes in the bulk $Fe^{3+}/\Sigma Fe$, their redox state, and affecting the partitioning of trace elements and the fractionation of O isotopes. Worldwide distributed metasomatized peridotites represent the ideal case study to investigate the role that crystal chemistry has on the O-isotope fractionation. We present mineral-chemical data of mantle peridotites from Tallante (Spain) such as major and trace elements, oxygen fugacity, and O-isotope data. Our results show that the O-isotope composition of volumetrically minor spinel in the residual mantle can be significantly affected by the oxidising metasomatic melts or fluids, likely implying that the oxidation of Fe^{2+} to Fe^{3+} favours ^{18}O uptake in spinel structure with respect to ^{16}O.

1 | Introduction

Fluids and melts that formed upon subduction and by partial melting of mantle rocks cause metasomatism and, therefore, redox reactions (Evans 2012; Cannaò and Malaspina 2018; Stagno and Fei 2020). This process influences the O-isotope composition ($\delta^{18}O$) of mantle minerals due to isotopic fractionation occurring between the (metasomatic) fluids and the interacting minerals. Silicate mantle minerals have $\delta^{18}O$ values of ~+ 5.2‰ ± 0.3‰ (Mattey et al. 1994), oxides (e.g., magnetite) of ~+3.5‰. Mantle metasomatism can make the $\delta^{18}O$ values slightly heavier (Eiler 2001; Bindeman 2008), while interaction with crustal silicate melts modifies the $\delta^{18}O$ to higher values than oceanic material (Dallai et al. 2019, 2022). While the correlation between the chemistry of mantle minerals and the local fo_2 is known (i.e., Mg# of Ol and Opx, Cr# and Mg# of Spl where Mg# and Cr# are the molar ratios Mg/(Mg + Fe) and Cr/(Cr + Al)), the relationship between $\delta^{18}O$ and fo_2 remains unexplored. A correlation between mineral Fe oxidation state and $\delta^{18}O$ is expected as the oxidation of Fe^{2+} to Fe^{3+} in redox-sensitive minerals (e.g., Spl) might result in different bonding environments with free oxygen diffused and incorporated into the crystal lattice. The correlation between $\delta^{57/54}Fe$ values, $Fe^{3+}/\Sigma Fe$ ratios, Cr# and fo_2 (Williams et al. 2004, 2005), and between the $\delta^{18}O$ values and Cr# (Perinelli et al. 2006) was reported for metasomatized mantle xenoliths from cratonic areas. Additionally, the $Cr\#_{Spl}$ traces several processes like melt extraction (Brunelli et al. 2006), melt/rock interaction (Brunelli and Seyler 2010; Brunelli et al. 2014), melt addition (Birner et al. 2021) and oxidative metasomatism (Marras et al. 2023), all of which might contribute differently to the O isotope fractionation and extent of oxidation.

In this study, we investigated four peridotite mantle xenoliths from Tallante (Southeast Spain), for which recent studies demonstrated the effect that slab-derived fluids have on the O isotope fractionation (Dallai et al. 2019, 2022). We investigated in-situ major and trace element compositions of the minerals (including those from vein and matrix of one peridotite sample) to reveal evidence of metasomatism. Thus, we combined $Fe^{3+}/\Sigma Fe$ measurements with the $\delta^{18}O$ data from the same minerals to explore a possible link. Finally, a potential relation between Cr# and $\delta^{18}O$ of Spl is tested comparing our data with Spl-lherzolites with different provenance like Northern Victoria Land (Antarctica) and Vitim (Siberia), Yitong (NE China), Rio Puerco (New Mexico) and Vema (Mid-Atlantic Ridge).

2 | Materials and Methods

We analysed three representative samples of (Pl-)Spl bearing lherzolites (TL14, TL45, TL53; Figure S1a–f) and one composite Pl-Spl harzburgite xenolith cut by a felsic vein (TL112; Figure 1 and Figure S1g–i) from Tallante, whose detailed geological setting and petrographic information are given in the Data S1 along with the description of the analytical techniques. We present single crystal analyses of Spl, Opx, Cpx, and Ol extracted from the selected rocks and the vein of TL112 (Figure S3). Our collected data were then compared with those of differently metasomatized mantle peridotites such as those from Northern Victoria (Perinelli et al. 2006, 2012) and Vitim (Ionov et al. 1993) peridotites, the only studies for which $Cr\#_{Spl}$, $Mg\#_{Ol}$, $Fe^{3+}/\Sigma Fe_{Spl}$ and mineral $\delta^{18}O$ are available to achieve the scope of this study, that is, exploring the crystal-chemical effect on the O-isotope fractionation in minerals. Noteworthy, samples BR218 and BR219 from Northern Victoria Land are composite with an amphibole-bearing vein (2 mm wide) that cuts the lherzolite and a cumulate wehrlite that adheres to a coarse-grained harzburgite, respectively (Perinelli et al. 2014).

3 | Results and Discussion

3.1 | Mineral Chemistry and Oxygen Fugacity of Tallante Peridotites With Respect to Literature Data

3.1.1 | Major Elements

The major elements composition of mineral from TL14 and TL53, along with data for TL112 (Bianchini et al. 2015) and TL45 (Beccaluva et al. 2004) are reported in Table S1 along with Northern Victoria and Vitim peridotites used to evaluate the potential link between crystal chemistry and O-isotope fractionation. Compositional maps (Figure S4) show core-to-rim homogeneity for the selected Spl from TL14, TL45, and TL112, as well as for Cpx and Opx grains from the peridotite matrix and vein of TL112.

The $Mg\#_{Ol}$ for the four Tallante peridotites is 0.90 ± 0.01 (Figure 2). Their composition overlaps with the $Mg\#_{Ol}$ from Northern Victoria (0.89 ± 0.02) and Vitim (0.90 ± 0.01). The $Mg\#_{Opx}$ of 0.90 ± 0.01 in Tallante peridotites is consistent with that of Northern Victoria and Vitim of 0.90–0.91 and 0.90–0.92, respectively. The Cpx from our Tallante peridotites is diopsidic with Cr_2O_3 content of 0.92–1.25 wt%, TiO_2 of 0.33–0.86 wt%, Na_2O of 0.55–0.88 wt%, and FeO of 2.14–2.35 wt% (Table S1) like Northern Victoria and Vitim Cpx, except for Na_2O, which is slightly higher (0.78–1.42 wt% and 0.91–2.24 wt%, respectively). The $Cr\#_{Spl}$ is consistent between our investigated samples and Northern Victoria, being 0.139–0.187 and 0.108–0.193, respectively (Figure 2) and similar to Vitim Spl peridotites (0.080–0.343), but distinct from two Vitim samples reporting the occurrence of both Spl and Grt, for which the values are 0.204 and 0.210.

3.1.2 | Trace Elements

The trace element compositions of Ol, Opx, and Cpx were analysed in-situ in TL14, Cpx in TL45, Opx and Cpx in TL53, and only

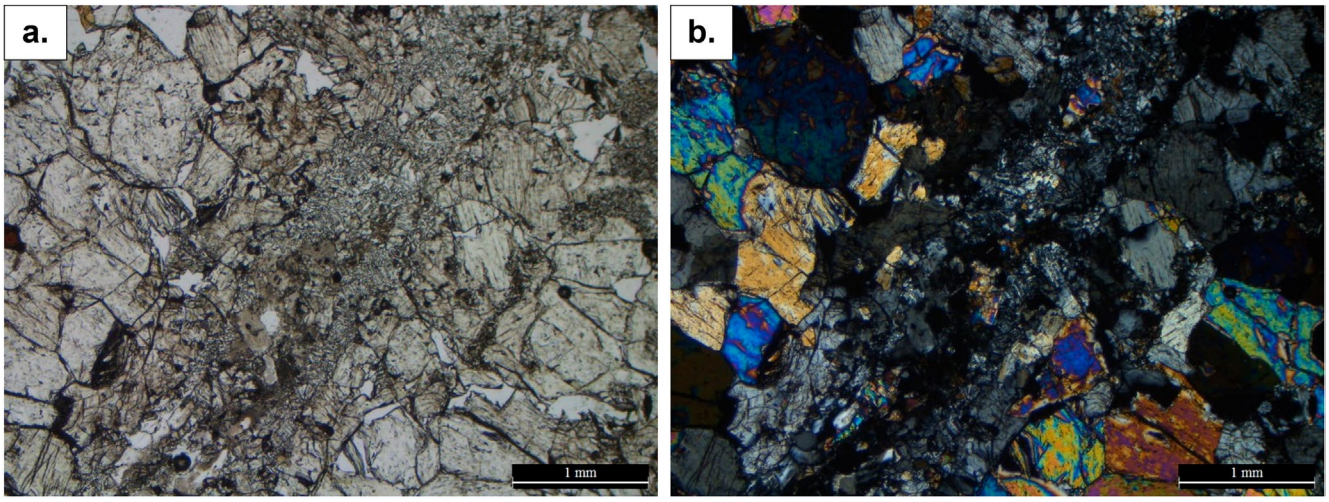

FIGURE 1 | Polarised transmitted light micrographs of TL112 doubled polished section. (a) plane-polarised light; (b) crossed polarised light. The sample shows the felsic vein with Pl and Px. Pl, plagioclase; Px, pyroxene; Spl, spinel. [Colour figure can be viewed at wileyonlinelibrary.com]

Opx in TL112 samples (Table S2) and compared with those from Northern Victoria Land and Vitim for the same reasons discussed above. The Cpx shows incompatible element concentrations like those from Northern Victoria Land and Vitim (Perinelli et al. 2006; Ionov, Ashchepkov, et al. 2005; Ionov, Blichert-Toft, et al. 2005; Figure 3a). Both U and Th enrichments are observed. An evident Sr depletion ($Sr^* = Sr_N/[(Ce_N + Nd_N)/2] = 0.09$) is recorded only in TL14 and TL45 samples (Figure 3a). A slight Eu depletion ($Eu^* = Eu_N/[(Sm_N + Gd_N)/2] = 0.8$) is shown in Figure 3b that, coupled with Sr depletion, is indicative of Pl crystallisation also identified from petrographic investigation (Figure S1). The TL53 Cpx shows a flat REE pattern like unveined anhydrous peridotite xenoliths of Tallante (Figure 3b). As for Cpx, the Sr depletion ($Sr^* = 0.03–0.04$) in TL14 and TL112 Opx and the prominent Eu depletion ($Eu^* = 0.02$) in Opx from sample TL112 are due to Pl crystallisation (Figure 3c,d). Data for Tallante Opx (Figure 3c) are consistent with those available for Northern Victoria Land and Vitim, with REE pattern in TL112 Opx showing a significant HREE enrichment compared to the other samples (Figure 3d and Table S2). Olivine from sample TL14 shows enrichments in Li (5.83 ± 0.14 ppm).

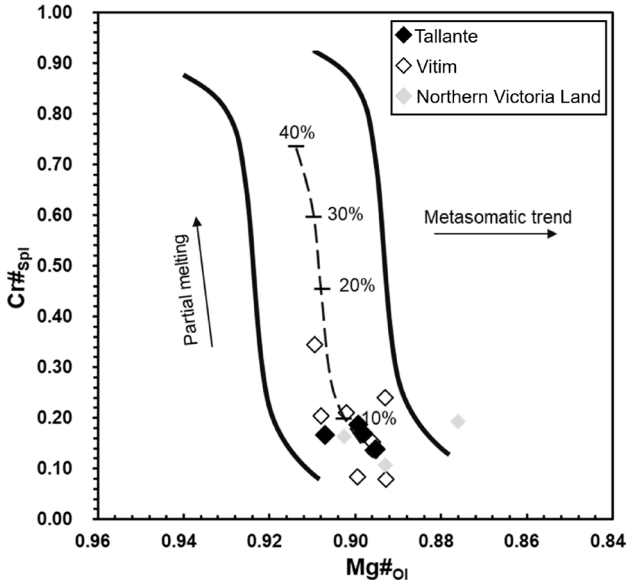

FIGURE 2 | $Cr\#_{Spl}$ plotted as function of $Mg\#_{Ol}$ for Tallante peridotites compared with literature data (see the text for the references). The Ol-Spl Mantle Array (OSMA) from Arai (1994) is reported along with trend of partial melting and metasomatism from Bonadiman et al. (2021).

3.1.3 | Iron Oxidation State of Analysed Opx, Cpx and Spl

The Mössbauer spectra for Spl, Cpx, and Opx grains are shown in Figure 4a–g. The $Fe^{3+}/\Sigma Fe$ of Spl ranges from 0.10 and 0.14 (±0.02). These values are lower than those reported by Canil and O'Neill (1996) for mantle peridotites ($Fe^{3+}/\Sigma Fe = 0.15–0.29$), but in agreement with $Fe^{3+}/\Sigma Fe$ ratios of

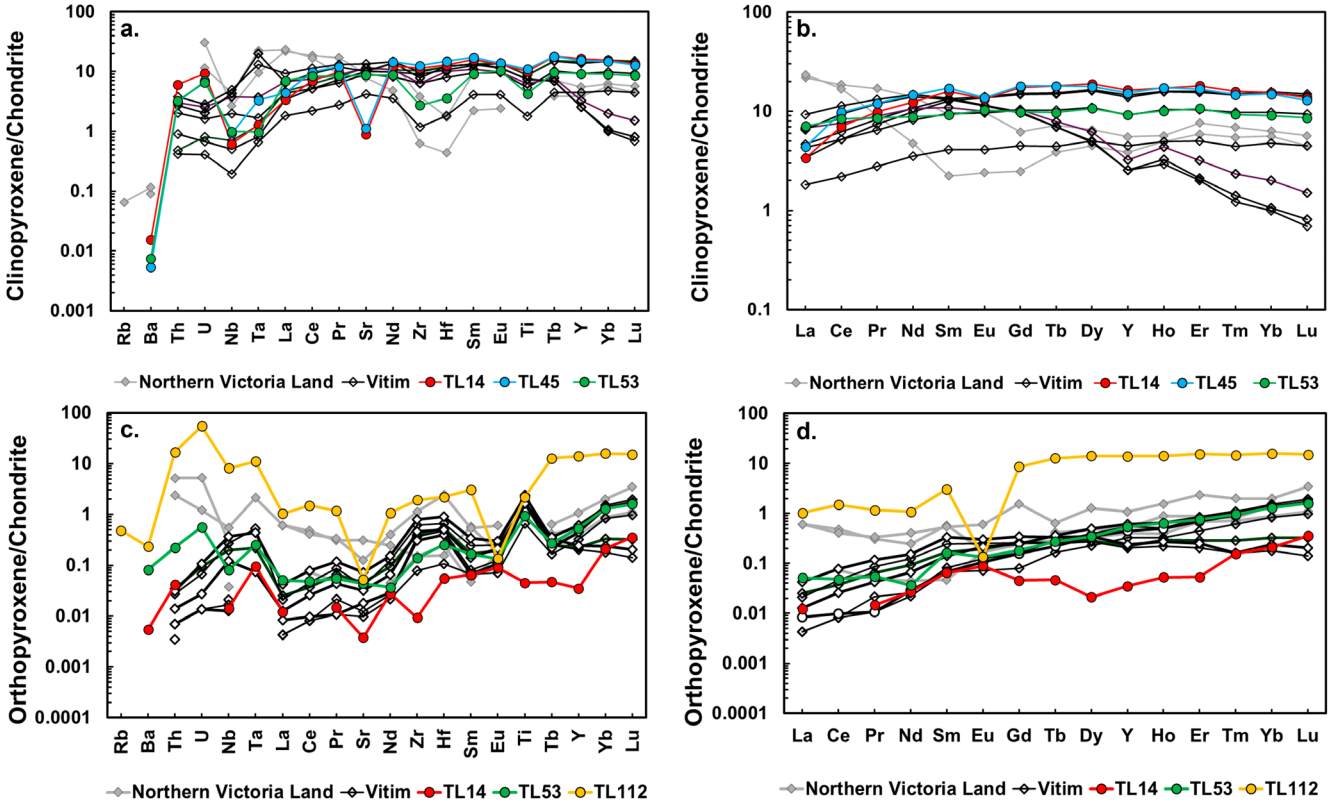

FIGURE 3 | (a) Chondrite-normalised trace element pattern of TL14, TL45, TL53 Cpx. (b) Chondrite-normalised Rare Earth Element pattern of TL14, TL45, TL53 Cpx. (c) Chondrite-normalised trace element pattern of TL14, TL53, TL112 Opx. (d) Chondrite-normalised Rare Earth Element pattern of TL14, TL53, TL112 Opx. The TL112 Opx represents the average of orthopyroxenes in contact with the felsic vein (Opx1a, Opx2a, Opx3a, Opx4a in Table S2). The normalised trace element patterns are compared with Northern Victoria Land and Vitim samples. Normalising values from McDonough and Sun (1995). [Colour figure can be viewed at wileyonlinelibrary.com]

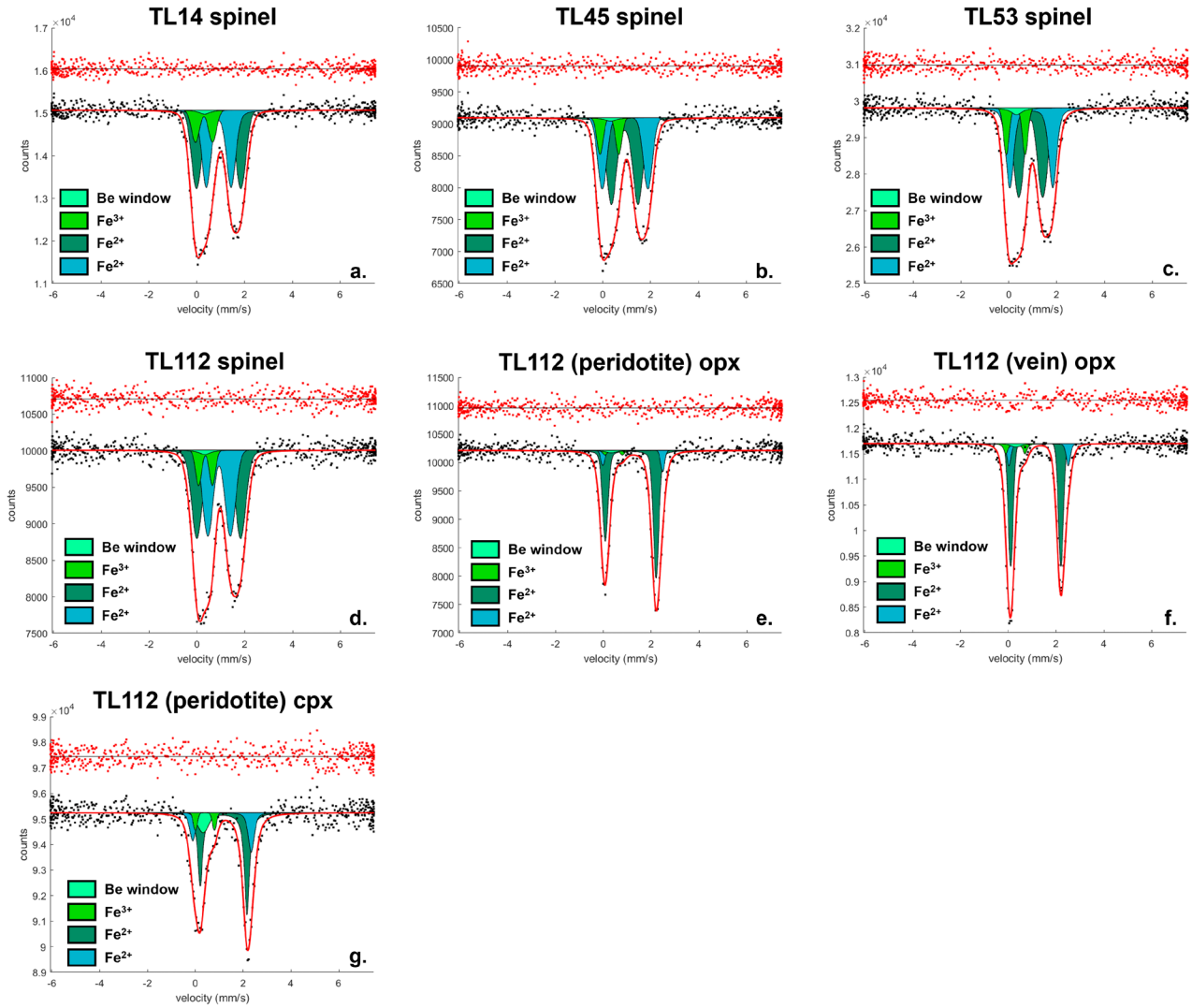

FIGURE 4 | Mössbauer spectra (a–g) of minerals from Tallante peridotite samples. The notation *peridotite* refers to those spectra acquired in minerals from the peridotitic matrix while the notation *vein* refers to minerals from felsic vein. [Colour figure can be viewed at wileyonlinelibrary.com]

some Vitim and Northern Victoria Land samples (Table 1). The $Fe^{3+}/\Sigma Fe$ of Opx from TL112 vein is higher than that measured in Opx from the matrix, with values of 0.08 and 0.03 (±0.02), respectively. The Cpx has $Fe^{3+}/\Sigma Fe$ ratio of 0.08 (±0.03) that is much lower than the averaged peridotitic Cpx of 0.22 (±0.07; Canil and O'Neill 1996).

3.1.4 | Determination of Tallante Peridotites fo_2

The estimated fo_2 ranges from −1.5 and −1.1 log units (±0.6) normalised to the fayalite-magnetite-quartz buffer (FMQ). This fo_2 falls within the range proposed by Schettino et al. (2023) for sulfide-bearing mantle xenoliths from Tallante, by Bénard et al. (2018) for subduction-metasomatised lithospheric mantle and by Frost and McCammon (2008) relative to massifs peridotites from Beni Bousera and Ronda.

3.2 | $\delta^{18}O$ of Spl, Cpx, Opx and Ol From Metasomatized Tallante Peridotites

The $\delta^{18}O$ of Spl, Opx, Cpx and Ol from the studied Tallante samples are from Dallai et al. (2019); (Table 1 and Table S4). In particular, $\delta^{18}O_{spl}$ ranges from +4.2 (TL112 matrix) and +5.1‰ (TL14). Both Cpx and Opx show heavier $\delta^{18}O$ values up to +6.5‰, while Ol ranges from +5.2 (TL14) to +5.7‰ (TL112). The $\delta^{18}O$ measured in Opx from the TL112 felsic vein shows a higher value of +9.8‰.

3.3 | Geochemical Evidence of Metasomatism

Figure 2 allows us to constrain metasomatic and melting processes capable of causing the Cr# variability plotted against the $Mg\#_{Ol}$ with respect to the Ol-Spl mantle array (OSMA trend; Arai 1994).

TABLE 1 | Rock type, P, T, logfo_2 (ΔFMQ), #Mg_{Ol}, #Cr_{Spl}, $Fe^{3+}/\sum Fe_{Spl}$, $\delta^{18}O_{Spl}$ of Tallante (this study), Vitim and Northern Victoria Land samples.

Locality	Sample	Rock type	P (GPa)	T (°C)	logfo_2 (ΔFMQ) Ballhaus et al. (1991)	#Mg_{Ol}	#Cr_{Spl}	$Fe^{3+}/\sum Fe_{Spl}$	$\delta^{18}O_{Spl}$
Tallante (subduction-related/collisional xenoliths)									
This study									
	TL 14	Pl-Spl lherzolite	0.8	1000	−1.07	0.898	0.170	0.14	+5.1[a]
	TL 53	Pl-Spl lherzolite	0.8	1000	−1.19	0.907	0.167	0.14	+4.5[a]
	TL 45	Pl-Spl lherzolite	0.8	1000	−1.29	0.899	0.187	0.12	+4.4[a]
	TL 112 matrix	Composite harzburgite[b]	0.8	1000	−1.49	0.895	0.139	0.10	+4.2[a]
Vitim (cratonic xenoliths)									
Ionov et al. (1993, 1994); Goncharov and Ionov (2012)									
	314–56	Spl lherzolite	1.5	818	*−1.12*	0.893	0.080	0.13	
	314–58	Spl lherzolite	1.4	775	*−0.69*	0.899	0.084	0.14	+5.4
	314–5	Spl lherzolite	2.1	1055	*0.07*	0.893	0.240	0.29	
	314–6	Spl lherzolite	1.9	1006	*−1.32*	0.909	0.343	0.15	+5.1
	314–59	Spl lherzolite	2.1	1061	*−0.78*	0.896	0.153	0.21	
	314–230	Spl-Grt lherzolite	2.1	1077	*−0.48*	0.902	0.210	0.22	
	314–580	Spl-Grt lherzolite	2.2	1096	*−0.48*	0.908	0.204	0.24	+4.9
Northern Victoria Land (cratonic xenoliths)									
Perinelli et al. (2006, 2012)									
	GP42	Spl lherzolite	1.6	1113	*−1.20*	0.893	0.108	0.22	+4.9
	BR218	Composite lherzolite[c]	0.9	981	*−1.14*	0.876	0.193	0.14	+4.4
	BR219	Composite harzburgite[d]	1.2	1047	*−1.27*	0.903	0.164	0.14	+3.8

Note: In italics logfo_2 data for literature samples re-calculated in this study using Ballhaus et al. (1991) oxythermobarometer.
[a]$\delta^{18}O_{Spl}$ as reported by Dallai et al. (2019).
[b]Harzburgite crosscut by felsic vein (Pl + Opx).
[c]Lherzolite crosscut by an amphibole-bearing vein (Perinelli et al. 2012).
[d]A cumulate wehrlite that adheres to a coarse-grained harzburgite (Perinelli et al. 2012).

Analyses of metasomatized mantle peridotites from Tallante, Vitim and Northern Victoria are all plotted, despite their complex and distinct petrological history, as the $Cr\#_{Spl}$ is used to assess the potential link between crystal chemistry and O-isotope fractionation.

Partial melting and melt extraction processes are usually constrained by the analyses of trace elements in pyroxene of peridotites, with the former causing LREE depletion (i.e., $La_N/Yb_N < 1$), with respect to metasomatism that causes LREE enrichment (i.e., $La_N/Yb_N > 1$) (Avanzinelli et al. 2020).

In TL112 harzburgite, an enrichment in LREE can be observed in the Opx close to the felsic vein (Figure 5), a proof of the metasomatic event(s). In fact, the complex multi-stage history of partial melting and metasomatism of the subcontinental lithospheric mantle from which Tallante xenoliths are from has been a matter of investigation by several authors (Beccaluva et al. 2004; Shimizu et al. 2008; Rampone et al. 2010; Bianchini et al. 2011, 2015; Hidas et al. 2016; Marchesi et al. 2017; Schettino et al. 2021).

3.4 | Modelled C-O-H Fluids Speciation

At the given P, T, and f_{O2} of Tallante samples, the thermodynamic modelling for C-O-H fluid of Zhang and Duan (2009)

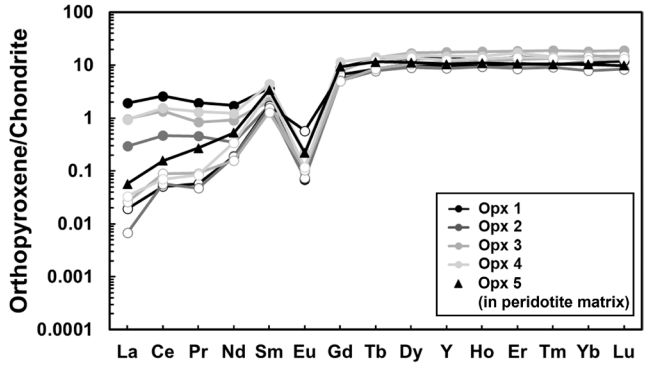

FIGURE 5 | Chondrite-normalised (McDonough and Sun 1995) Rare Earth Element pattern of TL112 Opx as reported in Table S2. For each Opx analysed, the point of analysis in contact with the felsic vein (filled symbols) and the point far from the vein (empty symbols) were reported. The REE concentration for the Opx in peridotite matrix (filled triangle) is the mean of five analysis points (see Table S2).

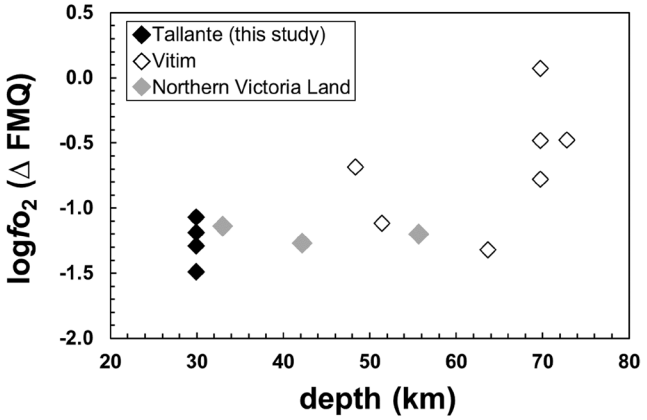

FIGURE 6 | Diagram of Tallante $\Delta \log fo_2$ (FMQ) data versus depth (km) compared with literature Spl-peridotites from Northern Victoria Land and Vitim cratons (see references in the text).

predicts the coexistence with CO_2-H_2O-bearing fluids at graphite saturation in line with the findings of Dallai et al. (2022) who described the occurrence of H_2O-rich rhyolitic melt inclusions in the Opx of TL112 sample reaction zone, along with graphite in felsic veins and in the Opx-rich reaction zones found in other Tallante peridotites (Bianchini and Natali 2017).

In Figure 6 the fo_2 data are compared as a function of equilibrated depth along with literature values for cratonic peridotites from Vitim (Ionov et al. 1993, 1994; Goncharov and Ionov 2012) and Northern Victoria Land (Perinelli et al. 2006, 2012). For consistency, the $\log fo_2$ of literature Vitim and Northern Victoria Land cratonic xenoliths was re-calculated employing the same oxythermobarometer.

The Tallante Pl-Spl peridotites exhibit fo_2 conditions that overlap with those estimated for Northern Victoria Land xenoliths (Perinelli et al. 2012, 2014; Martin et al. 2015) and stand at the lower end compared to samples from subduction-related metasomatized lithospheric mantle (Bénard et al. 2018).

3.5 | The Effect of Metasomatism on $\log fo_2$, Fe^{3+} and $\delta^{18}O$

Deviations of $\delta^{18}O$ values of mantle minerals are due to their interaction with recycled oceanic (+continental) crust into the mantle source (Eiler 2001; Dallai et al. 2019; Cooper et al. 2004). In the case of Tallante samples, $\delta^{18}O$ values showed a limited compositional range among equilibrated mantle minerals (Table S4). In this view, equilibration T and time have dominant control on O-isotope composition of minerals, as metasomatic agents are generally highly reactive and limited to low volume fractions to produce widespread metasomatic effects in the peridotitic domain.

The fo_2 coupled with the $\delta^{18}O$ values available for Ol, Opx and Cpx (Figure 7a–c) of the studied peridotites shows no evident trend regardless of the provenance of the mantle peridotites. In contrast, the fo_2 correlates with the $\delta^{18}O$ values of Spl (Figure 7d), in particular in the case of Tallante samples. This is plausible considering that the chemistry of Spl has the main control on the fo_2 (Ballhaus et al. 1991). In turn, $Fe^{3+}/\Sigma Fe_{Spl}$ ratios (Figure 8a) and Fe^{3+} calculated as atoms per formula unit (apfu; Figure 8b) covariate positively with $\delta^{18}O_{spl}$ for Tallante and Northern Victoria Land peridotites despite their different geological settings supporting, therefore, a potential crystal-chemical effect. One out of three Vitim samples represents an outlier as a result of the Cr-rich nature of the Spl as evidenced in Figure 2. The correlation between fo_2 and $\delta^{18}O$ values of Spl might raise the question of whether decompression driven by asthenosphere upwelling following the edge delamination event of the Iberian continental margin in the Miocene (Duggen et al. 2005; Mancilla et al. 2015, 2018) would have caused the increase of fo_2 of Tallante peridotites. However, since the fo_2 is dominantly controlled by T and $Fe^{3+}/\Sigma Fe_{Spl}$, the lack of evidence in the P effect on ferric iron incorporation in Spl does not support this alternative explanation.

Magnetite is an important end-member component of mantle Spl for which it has been shown that cation diffusion rates depend on fo_2 due to internal redox reactions involving Fe^{2+} and Fe^{3+}, and to a transition from an interstitial diffusion mechanism at low fo_2 to a vacancy mechanism under more oxidising conditions (van Orman and Crispin 2010). Cations are distributed on distinct octahedral and tetrahedral sites, occupied primarily by Al^{3+} and Mg^{2+}, respectively. In addition, Spl has octahedral interstitial sites and two different types of tetrahedral interstitial sites. Mössbauer spectra indicate that Fe^{3+} in Tallante spinels is octahedrally coordinated. Figure 8a,b suggest that increasing oxidation of Fe^{2+} to Fe^{3+} occurs in conjunction with ^{18}O uptake in Spl structure. Obviously, the formulation of an accurate model would benefit from a more important dataset along with experiments conducted at high P and T and known $Fe^{3+}/\Sigma Fe$.

These observations, coupled with the positive Cr#-Fe^{3+} trend (Figure 9a), may suggest increasing interaction with (metasomatic) hydrous melt (Tallante) and/or fluids (Northern Victoria Land, Vitim) at depth. On the other hand, the $Cr\#_{Spl}$ also reflects the extent of partial melting at shallower depths. When a larger dataset is considered, including cratonic peridotites

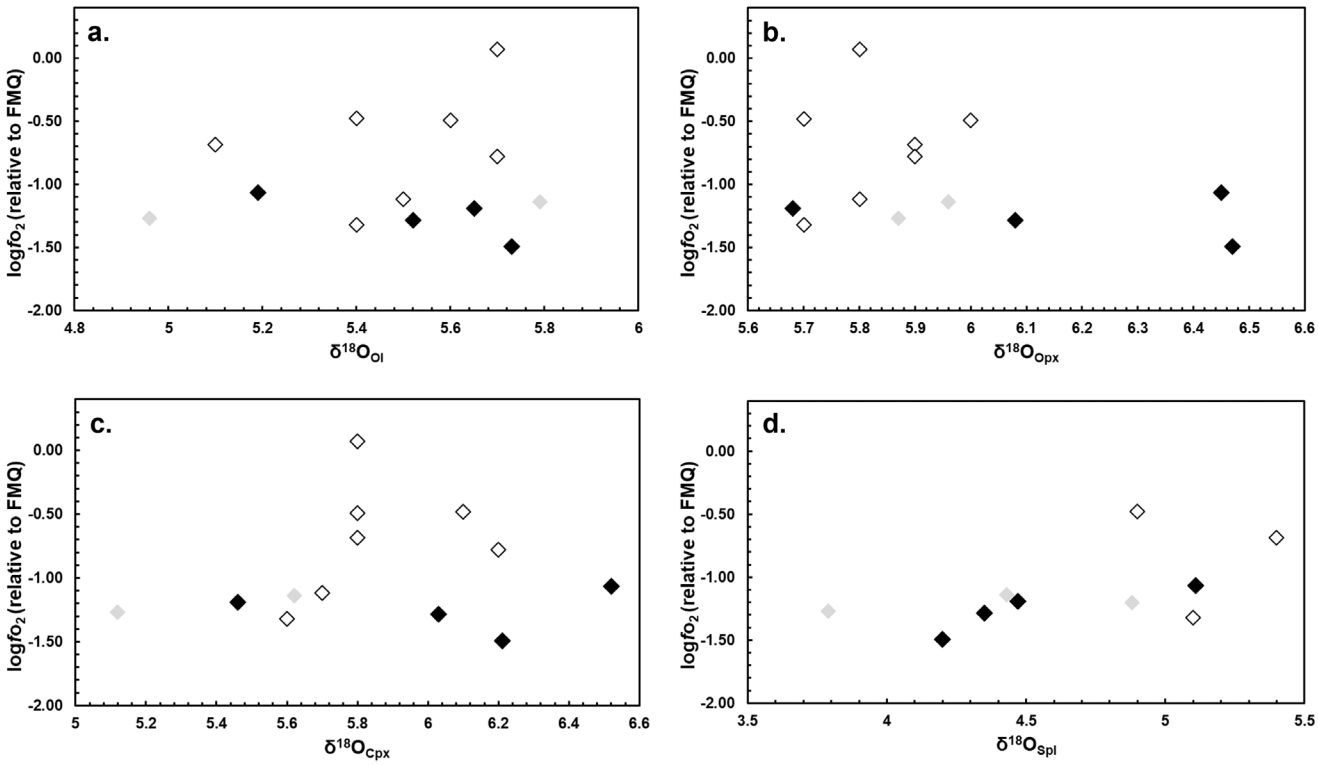

FIGURE 7 | $\Delta \log fo_2$ (FMQ) versus $\delta^{18}O$ for (a) Ol, (b) Opx, (c) Cpx and (d) Spl. A positive correlation in the case of Spl is observed for Tallante samples, while no preferential trends observed for Ol, Cpx and Opx. The $\delta^{18}O$ analytical error (1 S.D.) is 0.1‰.

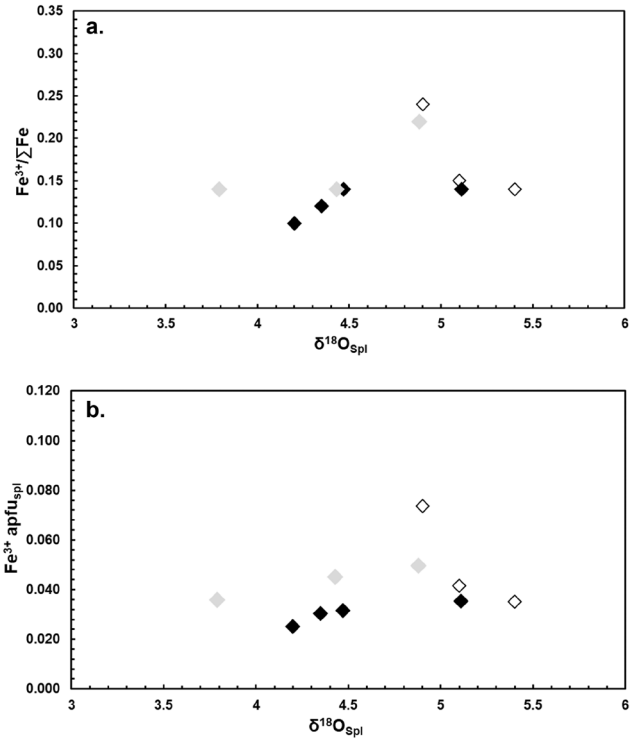

FIGURE 8 | (a) $Fe^{3+}/\Sigma Fe$ ratio versus $\delta^{18}O$ for Spl and (b) Fe^{3+} apfu for Spl versus $\delta^{18}O$. Legend as in Figure 7. The $\delta^{18}O$ analytical error (1 S.D.) is 0.1‰.

from Yitong (NE China; Xu et al. 1996), subduction xenoliths from Rio Puerco (New Mexico; Perkins et al. 2006; Porreca et al. 2006) and abyssal peridotites from Vema (Mid-Atlantic Ridge; Brunelli et al. 2006; Cipriani et al. 2009) (Table S5), the general negative trend in the Cr#-$\delta^{18}O_{spl}$ diagram (Figure 9b) seems to hold true, possibly reflecting the effects of partial melting on the production of liquids with higher $\delta^{18}O$ and, as a consequence, residues with lower $\delta^{18}O$. A similar mechanism has been proposed for $\delta^{18}O$ enrichment in basaltic glasses from Lau Basin, where the melting of a fertile mantle source was triggered by slab-derived fluids (Macpherson and Mattey 1998).

It may be possible that $\delta^{18}O$ of volumetrically minor Spl in the residual mantle is more influenced by (oxidising) metasomatic melt/fluid. In the case of the Tallante samples, the oxidising nature of the metasomatic agent represented by the felsic vein is supported by the $Fe^{3+}/\Sigma Fe$ ratios of Opx, which are 0.03 in the matrix and 0.08 in the vein, and the $\delta^{18}O$ values measured in Ol and Opx showing heavier values with respect to the vein.

4 | Conclusions

Tallante subduction xenoliths represent the ideal samples to investigate the effect of metasomatic fluids on mantle redox conditions, $Fe^{3+}/\Sigma Fe$ and $\delta^{18}O$ signature. We observed a positive correlation between fo_2 and $\delta^{18}O_{Spl}$ values, as well as between $Fe^{3+}/\Sigma Fe_{Spl}$, Fe^{3+} apfu and $\delta^{18}O_{Spl}$. These findings indicate that the O-isotope composition of Spl can be significantly affected by oxidising metasomatic melts or fluids in conjunction with the oxidation of Fe^{2+} to Fe^{3+}, that is during an increase in the bulk rock fo_2. However, more combined $Fe^{3+}/\Sigma Fe$ and $\delta^{18}O$ data are needed to better understand the effects of metasomatism at the crystal-chemical scale.

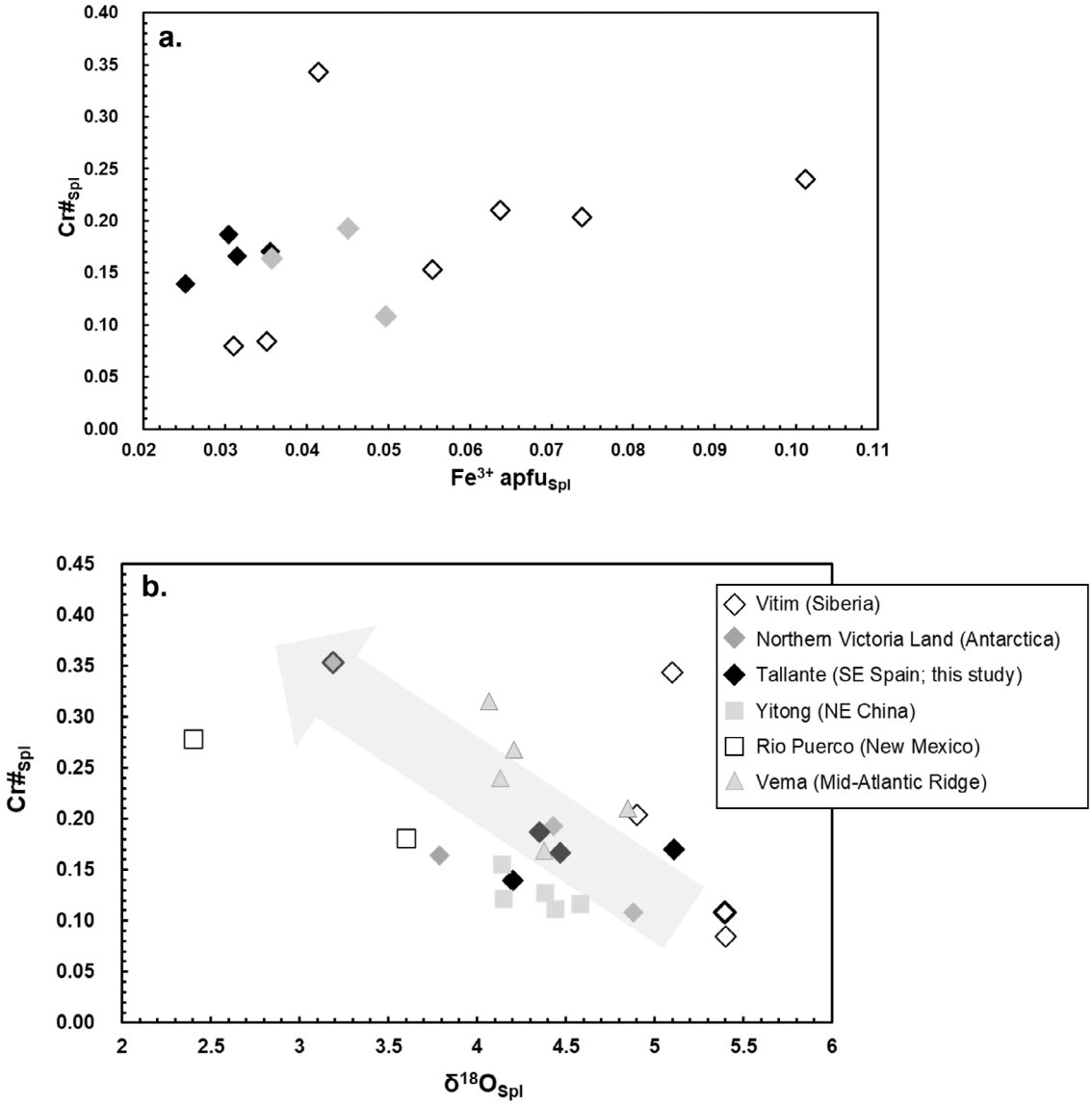

FIGURE 9 | (a) Cr# versus Fe^{3+} apfu and (b) Cr# vs. $\delta^{18}O$ for Spl from Tallante and literature (see reference in the text). Bold symbols for Northern Antarctica and Vitim are referred to samples GP-10 and 86–1, respectively, for which Spl $Fe^{3+}/\Sigma Fe$ was not measured, but $Cr\#_{Spl}$ and $\delta^{18}O_{spl}$ data are available in literature (the entire dataset is reported in Table S5). The arrow indicates the trend related to partial melting. The $\delta^{18}O$ analytical error (1 S.D.) is 0.1‰.

Acknowledgements

The authors greatly acknowledge Dr. Andrea Orlando and Eleonora Braschi from the MEMA laboratory of Florence for the EPMA analysis and Matteo Paciucci (IGAG-CNR) for SEM analysis with elements mapping. We also thank the ID18 beamline at ESRF (now ID14 at European Synchrotron Radiation Facility) for the in situ Mössbauer analysis and G. Sessa (University of Milan) for assistance during LA-ICP-MS sessions. This work was supported by a research scholarship from the Dr. Eduard Gübelin Association for Research & Identification of Precious Stones to G.M. V.S. acknowledges financial support by HERMES project n. 440 2022R35X8Z. MUR is acknowledged for the "Dipartimento di Eccellenza" 2018–2023 and 2023–2027, which supported trace element analyses at the University of Milano. Finally, the authors thank Prof. Ionov for sharing Vitim data, and Erwin Schettino and an anonymous reviewer for their constructive comments. The authors are grateful to editor Klaus Mezger for his meticulous final revision of the manuscript.

Open access publishing facilitated by Universita degli Studi di Roma La Sapienza, as part of the Wiley - CRUI-CARE agreement.

Conflicts of Interest

The authors declare no conflicts of interest.

Data Availability Statement

All data presented within the article and the Supporting Information—S1.

References

Arai, S. 1994. "Characterization of Spinel Peridotites by Olivine-Spinel Compositional Relationships: Review and Interpretation." *Chemical Geology* 113, no. 3–4: 191–204. https://doi.org/10.1016/0009-2541(94)90066-3.

Avanzinelli, R., G. Bianchini, M. Tiepolo, et al. 2020. "Subduction-Related Hybridization of the Lithospheric Mantle Revealed by Trace Element and Sr-Nd-Pb Isotopic Data in Composite Xenoliths From Tallante (Betic Cordillera, Spain)." *Lithos* 352: 105316. https://doi.org/10.1016/j.lithos.2019.105316.

Ballhaus, C., R. F. Berry, and D. H. Green. 1991. "High Pressure Experimental Calibration of the Olivine-Orthopyroxene-Spinel Oxygen Geobarometer: Implications for the Oxidation State of the Upper Mantle." *Contributions to Mineralogy and Petrology* 107: 27–40. https://doi.org/10.1007/BF00311183.

Beccaluva, L., G. Bianchini, C. Bonadiman, F. Siena, and C. Vaccaro. 2004. "Coexisting Anorogenic and Subduction-Related Metasomatism in Mantle Xenoliths From the Betic Cordillera (Southern Spain)." *Lithos* 75: 67–87. https://doi.org/10.1016/j.lithos.2003.12.015.

Bénard, A., K. Klimm, A. B. Woodland, et al. 2018. "Oxidising Agents in Sub-Arc Mantle Melts Link Slab Devolatilisation and Arc Magmas." *Nature Communications* 9: 3500. https://doi.org/10.1038/s41467-018-05804-2.

Bianchini, G., L. Beccaluva, G. M. Nowell, D. G. Pearson, and F. Siena. 2011. "Mantle Xenoliths From Tallante (Betic Cordillera): Insights Into the Multi-Stage Evolution of the South Iberian Lithosphere." *Lithos* 124: 308–318.

Bianchini, G., R. Braga, A. Langone, C. Natali, and M. Tiepolo. 2015. "Metasedimentary and Igneous Xenoliths From Tallante (Betic Cordillera, Spain): Inferences on Crust-Mantle Interactions and Clues for Post-Collisional Volcanism Magma Sources." *Lithos* 220: 191–199. https://doi.org/10.1016/j.lithos.2015.02.011.

Bianchini, G., and C. Natali. 2017. "Carbon Elemental and Isotopic Composition in Mantle Xenoliths From Spain: Insights on Sources and Petrogenetic Processes." *Lithos* 272: 84–91. https://doi.org/10.1016/j.lithos.2016.11.020.

Bindeman, I. 2008. "Oxygen Isotopes in Mantle and Crustal Magmas as Revealed by Single Crystal Analysis." *Reviews in Mineralogy and Geochemistry* 69, no. 1: 445–478. https://doi.org/10.2138/rmg.2008.69.12.

Birner, S. K., E. Cottrell, J. M. Warren, K. A. Kelley, and F. A. Davis. 2021. "Melt Addition to Mid-Ocean Ridge Peridotites Increases Spinel Cr# With no Significant Effect on Recorded Oxygen Fugacity." *Earth and Planetary Science Letters* 566: 116951. https://doi.org/10.1016/j.epsl.2021.116951.

Bonadiman, C., V. Brombin, G. B. Andreozzi, et al. 2021. "Phlogopite-Pargasite Coexistence in an Oxygen Reduced Spinel-Peridotite Ambient." *Scientific Reports* 11, no. 1: 11829. https://doi.org/10.1038/s41598-021-90844-w.

Brunelli, D., E. Paganelli, and M. Seyler. 2014. "Percolation of Enriched Melts During Incremental Open-System Melting in the Spine Field: A REE Approach to Abyssal Peridotites From the Southwest Indian Ridge." *Geochimica et Cosmochimica Acta* 127: 190–203. https://doi.org/10.1016/j.gca.2013.11.040.

Brunelli, D., and M. Seyler. 2010. "Asthenospheric Percolation of Alkaline Melts Beneath the St. Paul Region (Central Atlantic Ocean)." *Earth and Planetary Science Letters* 289: 393–405. https://doi.org/10.1016/j.epsl.2009.11.028.

Brunelli, D., M. Seyler, A. Cipriani, L. Ottolini, and E. Bonatti. 2006. "Discontinuous Melt Extraction and Weak Refertilization of Mantle Peridotites at the Vema Lithospheric Section (Mid-Atlantic Ridge)." *Journal of Petrology* 47, no. 4: 745–771. https://doi.org/10.1093/petrology/egi092.

Canil, D., and H. S. C. O'Neill. 1996. "Distribution of Ferric Iron in Some Upper-Mantle Assemblages." *Journal of Petrology* 37, no. 3: 609–635. https://doi.org/10.1093/petrology/37.3.609.

Cannaò, E., and N. Malaspina. 2018. "From Oceanic to Continental Subduction: Implications for the Geochemical and Redox Evolution of the Supra-Subduction Mantle." *Geosphere* 14, no. 6: 2311–2336. https://doi.org/10.1130/GES01597.1.

Cipriani, A., E. Bonatti, M. Seyler, et al. 2009. "A 19 to 17 ma Amagmatic Extension Event at the Mid-Atlantic Ridge: Ultramafic Mylonites From the Vema Lithospheric Section." *Geochemistry, Geophysics, Geosystems* 10, no. 10: Q10011. https://doi.org/10.1029/2009GC002534.

Cooper, K. M., J. M. Eiler, P. D. Asimow, and C. H. Langmuir. 2004. "Oxygen Isotope Evidence for the Origin of Enriched Mantle Beneath the Mid-Atlantic Ridge." *Earth and Planetary Science Letters* 220, no. 3–4: 297–316. https://doi.org/10.1016/S0012-821X(04)00058-5.

Dallai, L., G. Bianchini, R. Avanzinelli, et al. 2022. "Quartz-Bearing Rhyolitic Melts in the Earth's Mantle." *Nature Communications* 13: 7765. https://doi.org/10.1038/s41467-022-35382-3.

Dallai, L., G. Bianchini, R. Avanzinelli, C. Natali, and S. Conticelli. 2019. "Heavy Oxygen Recycled Into the Lithospheric Mantle." *Scientific Reports* 9: 8793. https://doi.org/10.1038/s41598-019-45031-3.

Duggen, S., K. Hoernle, P. van den Bogaard, and D. Garbe-Schönberg. 2005. "Post-Collisional Transition From Subduction-To Intraplate Type Magmatism in the Westernmost Mediterranean: Evidence for Continental-Edge Delamination of Subcontinental Lithosphere." *Journal of Petrology* 46: 1155–1201.

Eiler, J. M. 2001. "Oxygen Isotope Variations of Basaltic Lavas and Upper Mantle Rocks." *Reviews in Mineralogy and Geochemistry* 43, no. 1: 319–364. https://doi.org/10.2138/gsrmg.43.1.319.

Evans, K. A. 2012. "The Redox Budget of Subduction Zones." *Earth-Science Reviews* 113, no. 1–2: 11–32. https://doi.org/10.1016/j.earscirev.2012.03.003.

Frost, D. J., and C. A. McCammon. 2008. "The Redox State of the Earth's Mantle." *Annual Review of Earth and Planetary Sciences* 36: 389–420. https://doi.org/10.1146/annurev.earth.36.031207.124322.

Goncharov, A. G., and D. A. Ionov. 2012. "Redox State of Deep Off-Craton Lithospheric Mantle: New Data From Garnet and Spinel Peridotites From Vitim, Southern Siberia." *Contributions to Mineralogy and Petrology* 164: 731–745. https://doi.org/10.1007/s00410-012-0767-z.

Hidas, K., Z. Konc, C. J. Garrido, et al. 2016. "Flow in the Western Mediterranean Shallow Mantle: Insights From Xenoliths in Pliocene Alkali Basalts From SE Iberia (Eastern Betics, Spain)." *Tectonics* 35: 2657–2676. https://doi.org/10.1002/2016TC004165.

Ionov, D. A., I. Ashchepkov, and E. Jagoutz. 2005. "The Provenance of Fertile Off-Craton Lithospheric Mantle: Sr-Nd Isotope and Chemical Composition of Garnet and Spinel Peridotite Xenoliths From Vitim, Siberia." *Chemical Geology* 217, no. 1–2: 41–75. https://doi.org/10.1016/j.chemgeo.2004.12.001.

Ionov, D. A., I. V. Ashchepkov, H. G. Stosch, G. Witt-Eickschen, and H. A. Seck. 1993. "Garnet Peridotite Xenoliths From the Vitim Volcanic Field, Baikal Region: The Nature of the Garnet-Spinel Peridotite Transition Zone in the Continental Mantle." *Journal of Petrology* 34, no. 6: 1141–1175. https://doi.org/10.1093/petrology/34.6.1141.

Ionov, D. A., J. Blichert-Toft, and D. Weis. 2005. "Hf Isotope Compositions and HREE Variations in Off-Craton Garnet and Spinel Peridotite Xenoliths From Central Asia." *Geochimica et Cosmochimica Acta* 69, no. 9: 2399–2418. https://doi.org/10.1016/j.gca.2004.11.008.

Ionov, D. A., R. S. Harmon, C. France-Lanord, P. B. Greenwood, and I. V. Ashchepkov. 1994. "Oxygen Isotope Composition of Garnet and Spinel Peridotites in the Continental Mantle: Evidence From the Vitim Xenolith Suite, Southern Siberia." *Geochimica et Cosmochimica Acta* 58, no. 5: 1463–1470. https://doi.org/10.1016/0016-7037(94)90549-5.

Macpherson, C. G., and D. P. Mattey. 1998. "Oxygen Isotope Variations in Lau Basin Lavas." *Chemical Geology* 144, no. 3–4: 177–194. https://doi.org/10.1016/S0009-2541(97)00130-7.

Mancilla, F. d. L., G. Booth-Rea, D. Stich, et al. 2015. "Slab Rupture and Delamination Under the Betics and Rif Constrained From Receiver

Functions." *Tectonophysics* 663: 225–237. https://doi.org/10.1016/j.tecto.2015.06.028.

Mancilla, F. d. L., B. Heit, J. Morales, et al. 2018. "A STEP Fault in Central Betics, Associated With Lateral Lithospheric Tearing at the Northern Edge of the Gibraltar Arc Subduction System." *Earth and Planetary Science Letters* 486: 32–40. https://doi.org/10.1016/j.epsl.2018.01.008.

Marchesi, C., Z. Konc, C. J. Garrido, et al. 2017. "Multi-Stage Evolution of the Lithospheric Mantle Beneath the Westernmost Mediterranean: Geochemical Constraints From Peridotite Xenoliths in the Eastern Betic Cordillera (SE Spain)." *Lithos* 276: 75–89.

Marras, G., V. Stagno, G. B. Andreozzi, et al. 2023. "Extensive Oxidizing Events Recorded by Peridotite Mantle Xenoliths From the Hyblean Plateau: Evidence From Combined Measurements of Ferric Iron in Spinel With Noble Gases and Fluid Inclusions Chemistry in Olivine." *Lithos* 458-459: 107337. https://doi.org/10.1016/j.lithos.2023.107337.

Martin, A. P., R. C. Price, A. F. Cooper, and C. A. McCammon. 2015. "Petrogenesis of the Rifted Southern Victoria Land Lithospheric Mantle, Antarctica, Inferred From Petrography, Geochemistry, Thermobarometry and Oxybarometry of Peridotite and Pyroxenite Xenoliths From the Mount Morning Eruptive Centre." *Journal of Petrology* 56, no. 1: 193–226. https://doi.org/10.1093/petrology/egu075.

Mattey, D., D. Lowry, and C. Macpherson. 1994. "Oxygen Isotope Composition of Mantle Peridotite." *Earth and Planetary Science Letters* 128, no. 3–4: 231–241. https://doi.org/10.1016/0012-821X(94)90147-3.

McDonough, W. F., and S. S. Sun. 1995. "The Composition of the Earth." *Chemical Geology* 120, no. 3–4: 223–253. https://doi.org/10.1016/0009-2541(94)00140-4.

Perinelli, C., G. B. Andreozzi, A. M. Conte, R. Oberti, and P. Armienti. 2012. "Redox State of Subcontinental Lithospheric Mantle and Relationships With Metasomatism: Insights From Spinel Peridotites From Northern Victoria Land (Antarctica)." *Contributions to Mineralogy and Petrology* 164: 1053–1067. https://doi.org/10.1007/s00410-012-0788-7.

Perinelli, C., P. Armienti, and L. Dallai. 2006. "Geochemical and O-Isotope Constraints on the Evolution of Lithospheric Mantle in the Ross Sea Rift Area (Antarctica)." *Contributions to Mineralogy and Petrology* 151: 245–266. https://doi.org/10.1007/s00410-006-0065-8.

Perinelli, C., F. Bosi, G. B. Andreozzi, A. M. Conte, and P. Armienti. 2014. "Geothermometric Study of Cr-Spinels of Peridotite Mantle Xenoliths From Northern Victoria Land (Antarctica)." *American Mineralogist* 99, no. 4: 839–846. https://doi.org/10.2138/am.2014.4515.

Perkins, G. B., Z. D. Sharp, and J. Selverstone. 2006. "Oxygen Isotope Evidence for Subduction and Rift-Related Mantle Metasomatism Beneath the Colorado Plateau–Rio Grande Rift Transition." *Contributions to Mineralogy and Petrology* 151: 633–650. https://doi.org/10.1007/s00410-006-0075-6.

Porreca, C., J. Selverstone, and K. Samuels. 2006. "Pyroxenite Xenoliths From the Rio Puerco Volcanic Field, New Mexico: Melt Metasomatism at the Margin of the Rio Grande Rift." *Geosphere* 2, no. 7: 333–351.

Rampone, E., R. L. M. Vissers, M. Poggio, M. Scambelluri, and A. Zanetti. 2010. "Melt Migration and Intrusion During Exhumation of the Alboran Lithosphere: The Tallante Mantle Xenolith Record (Betic Cordillera, SE Spain)." *Journal of Petrology* 51, no. 1–2: 295–325. https://doi.org/10.1093/petrology/egp061.

Schettino, E., J. M. González-Jiménez, C. Marchesi, et al. 2023. "Mantle-To-Crust Metal Transfer by Nanomelts." *Communications Earth & Environment* 4: 256. https://doi.org/10.1038/s43247-023-00918-y.

Schettino, E., C. Marchesi, J. M. González-Jiménez, et al. 2021. "Metallogenic Fingerprint of a Metasomatized Lithospheric Mantle Feeding Gold Endowment in the Western Mediterranean Basin." *GSA Bulletin* 134, no. 5–6: 1468–1484. https://doi.org/10.1130/B36065.1.

Shimizu, Y., S. Arai, T. Morishita, and Y. Ishida. 2008. "Origin and Significance of Spinel-Pyroxene Symplectite in Lherzolite Xenoliths From Tallante, SE Spain." *Mineralogy and Petrology* 94: 27–43.

Stagno, V., and Y. Fei. 2020. "The Redox Boundary of Earth's Interior." *Elements* 16: 167–172. https://doi.org/10.2138/gselements.16.3.167.

van Orman, J. A., and K. L. Crispin. 2010. "Diffusion in Oxides." *Reviews in Mineralogy and Geochemistry* 72, no. 1: 757–825. https://doi.org/10.2138/rmg.2010.72.17.

Williams, H. M., C. A. McCammon, A. H. Peslier, et al. 2004. "Iron Isotope Fractionation and the Oxygen Fugacity of the Mantle." *Science* 304: 1656–1659.

Williams, H. M., A. H. Peslier, C. McCammon, et al. 2005. "Systematic Iron Isotope Variations in Mantle Rocks and Minerals: The Effects of Partial Melting and Oxygen Fugacity." *Earth and Planetary Science Letters* 235, no. 1–2: 435–452. https://doi.org/10.1016/j.epsl.2005.04.020.

Xu, Y. G., M. A. Menzies, D. P. Mattey, D. Lowry, B. Harte, and R. W. Hinton. 1996. "The Nature of the Lithospheric Mantle Near the Tancheng-Lujiang Fault, China: An Integration of Texture, Chemistry and O-Isotopes." *Chemical Geology* 134, no. 1–3: 67–81. https://doi.org/10.1016/S0009-2541(96)00081-2.

Zhang, C., and Z. Duan. 2009. "A Model for C–O–H Fluid in the Earth's Mantle." *Geochimica et Cosmochimica Acta* 73, no. 7: 2089–2102.

Supporting Information

Additional supporting information can be found online in the Supporting Information section.